

- 1 – The image contains 1966 pixels in the across-scan ("vertical") direction, which is the full CCD height. Each pixel measures 30  $\mu\text{m}$  across-scan and spans 176.8 mas on the sky. The readout direction is from top to bottom. Gaia's astrometric focal plane contains 7 rows of CCDs in the across-scan direction.
- 2 – The image contains 1700 pixels in the along-scan ("horizontal") direction. Each pixel measures 10  $\mu\text{m}$  along-scan and spans 58.9 mas on the sky. Gaia's CCDs are operated in Time-Delayed-Integration (TDI) mode, meaning that the charges in the CCD are transferred at the same speed as the optical image, the motion of the latter being driven by the slow scan of the spacecraft over the sky. Along-scan pixels are also referred to as TDI lines. The 1700 pixels displayed here correspond to 1.7 seconds of scanning time, one pixel lasting  $\sim 1$  millisecond. The full CCD has 4500 along-scan pixels, corresponding to 4.4 seconds of scanning and integration. Gaia's astrometric focal plane contains 9 strips of CCDs in the along-scan direction.
- 3 – The CCD has 15 non-illuminated pre-scan pixels, physically located between the serial register and the read-out node. These pixels are used for CCD-offset-level monitoring.
- 4 – The green "+" signs indicate sources simulated by the Gaia Instrument and Basic Image Simulator (GIBIS). The barely-visible number above each "+" sign indicates the Gaia G magnitude. The faintest source simulated by GIBIS has  $G = 22$  mag. Stars in the user-defined source list fainter than this limit are ignored by GIBIS.
- 5 – In order to comply with CCD-noise and telemetry-volume requirements, the CCDs are not read out in full frame but in window mode. Around each detected star, a small window is defined which is tracked throughout the focal plane. Only pixels within the windows are read out and transmitted to ground. Pixels between windows are flushed. The window size, as well as the sampling/binning strategy of pixels inside the window, depends on the star magnitude as well as on the CCD. For the astrometric instrument, and for the AF2 CCD depicted here, the along-scan ("horizontal") window size is 18 pixels for the brightest stars ( $G < 16$  mag) and 12 pixels for stars fainter than  $G = 16$  mag. Flux losses caused by the finite window size are corrected in the photometric ground processing.
- 6 – For windows in the astrometric AF2 CCD depicted here, all 12 pixels in the across-scan direction are binned together on chip, without introduction of additional noise, for stars fainter than  $G = 13$  mag. For brighter stars, there is no across-scan binning and windows have full pixel resolution. The post-mission on-ground data processing combines all one-dimensional transit measurements into an Astrometric Global Iterative Solution (AGIS), resulting in five-dimensional astrometric data – positions, parallaxes, and proper motions – for all stars.
- 7 – The maximum number of samples that can be observed simultaneously, i.e., per along-scan pixel (TDI line), is 24; this limit is defined by the Gaia scanning speed as well as by CCD-noise requirements. If two full-pixel resolution windows have simultaneously been assigned, there is temporarily no room for observing faint(er) stars. This explains the non-windowed stars in the vertical band above and below the centre of the cluster, where two bright-star windows have been allocated.
- 8 – The first sample in every window is preceded by a (single-pixel) braking sample. This sample is read (as opposed to flushed) and subsequently discarded on board. The braking sample largely absorbs an electronic instability in the CCD offset level caused by the transition between fast flushing of useless pixels and slow reading of useful pixels (reading is  $\sim 100$  times slower than flushing).
- 9 – Galactic cosmic rays, with typical energies at the GeV level, continuously hit the CCD at an approximate rate of 3 events per second per  $\text{cm}^2$  (the CCD active area is  $26.5 \text{ cm}^2$  and the integration time is 4.4 s). Cosmic rays can generate thousands of electrons in the CCD and can, depending on the angle of incidence, yield long stripes. The on-board software has a cosmic-ray filter preventing the spurious assignment of observation windows.
- 10 – The integration time of Gaia's CCDs can temporarily be reduced through activation of a TDI gate. This is useful to avoid the saturation of bright-star images. TDI gates will be used for all stars with  $G < 12$  mag during the length of their window (18 along-scan pixels). The activation of a gate affects the entire CCD. Faint stars observed simultaneously with the bright star hence also get a reduced integration time. Blue lines indicate the activation or release of a TDI gate.
- 11 – In case of overlapping windows, the on-board software leaves the highest-priority window, i.e., the window of the brightest star, in tact and truncates the samples of the lowest-priority window. In the on-ground processing, the overlapping windows are treated together, which enables proper de-blending.
- 12 – Gaia's two telescopes have non-rectangular apertures measuring  $1.45 \text{ m} \times 0.50 \text{ m}$  (ratio 3:1). The particular point-spread function generated by these mirrors is precisely matched by the non-rectangular pixel size, which is  $10 \mu\text{m} \times 30 \mu\text{m}$  (ratio 1:3). The image displayed here renders every non-rectangular pixel as square, which explains the "vertically" flattened shape of the cluster.
- 13 – In this example, the pixel-level HST image – including stars as well as background – has been directly passed as input to GIBIS. The Gaia on-board object-detection software properly assigns windows to a large number of objects, despite the fact that the HST Point-Spread Function (PSF) is systematically different from the Gaia one, in size, shape, and sampling. Those stars which have not received windows are either too faint ( $G > 20$  mag) or have a PSF which is not sufficiently Gaia-like. These results suggest that real-sky background inhomogeneities do not hamper Gaia's object-detection capabilities.

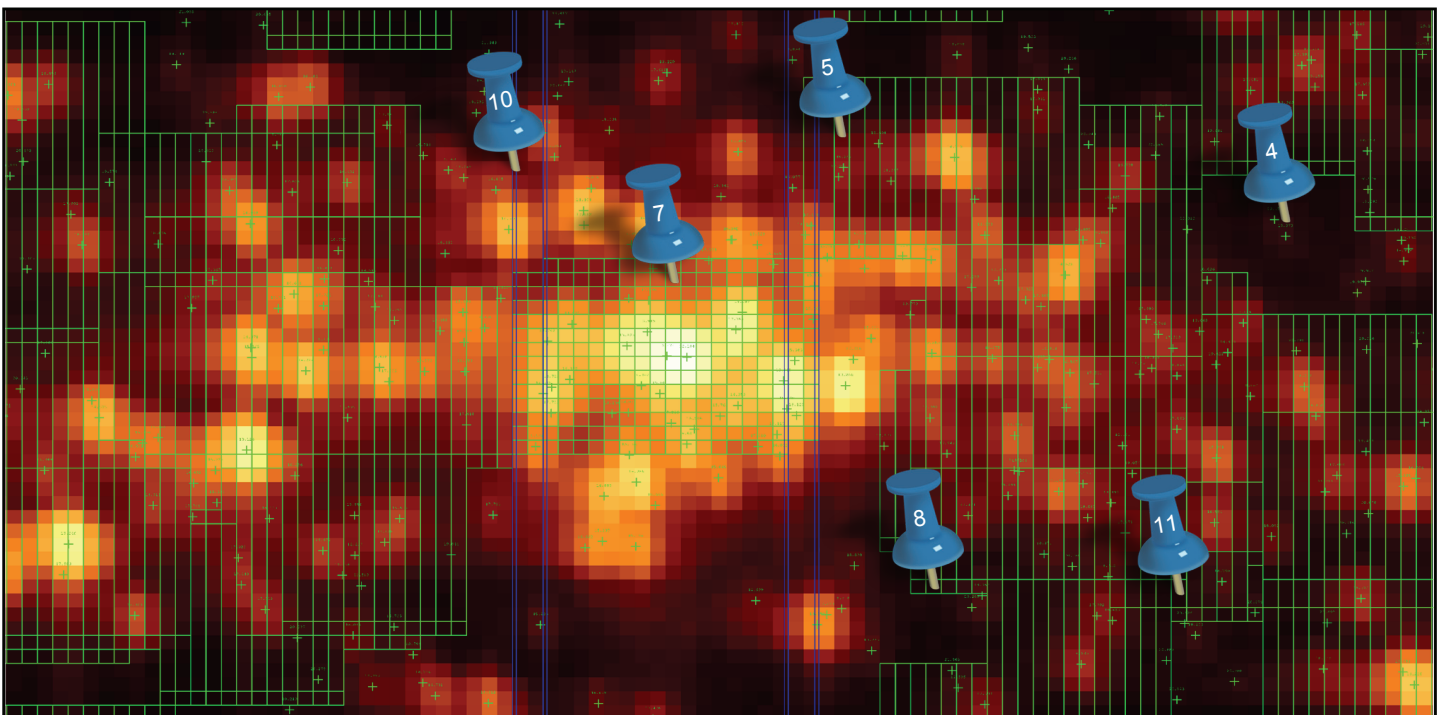


Figure – High-resolution view of the core of the R136 cluster, with Gaia observation windows (green boxes) superimposed on the HST-based image (heatmap).